

Using data and model to infer climate and environmental changes during the Little Ice Age in tropical West Africa

Anne-Marie Lézine¹, Maé Catrain¹, Julián Villamayor^{1,2} and Myriam Khodri¹.

1. Laboratoire d'Océanographie et du Climat. Expérimentation et Approche numérique/IPSL. Sorbonne Université-CNRS-IRD-MNHN. 4 Place Jussieu. 75005. Paris. France

2. Department of Atmospheric Chemistry and Climate, Institute of Physical Chemistry Rocasolano, CSIC, Madrid, Spain.

Abstract

Here we present hydrological and vegetation paleo-data extracted from 28 sites in West Africa from 5° S to 19° N and the past1000/PMIP4 IPSL-CM6A-LR climate model simulations covering the 850-1850 CE period to document the environmental and climatic changes that occurred during the Little Ice Age (LIA). The comparison between paleo-data and model simulations shows a clear contrast between the area spanning the Sahel and the Savannah in the North, characterized by widespread drought, and the equatorial sites in the South, where humid conditions prevailed. Particular attention was paid to the Sahel, whose climatic evolution was characterized by a progressive drying trend between 1250 and 1850CE. Three major features are highlighted: (1) the detection of two early warning signals around 1170 and 1240CE preceding the onset of the LIA drying trend; (2) an irreversible tipping point at 1800-1850CE characterized by a dramatic rainfall drop and a widespread environmental degradation in the Sahel; and (3) a succession of drying events punctuating the LIA, the major of which was dated around 1600CE. The climatic long-term evolution of the Sahel is associated with a gradual southward displacement of the Inter-Tropical Convergence Zone induced by the radiative cooling impacts of major volcanic eruptions that have punctuated the last millennium.

1. Introduction

Precipitation in tropical West Africa is closely related to the West African Monsoon (WAM) system, created by the temperature land-sea contrast between the tropical Atlantic and the west of the African continent (Nicholson 2013) and is also influenced by the migration of the Inter Tropical Convergence Zone (ITCZ, Gagdil 2018). The WAM long-term variability during the 20th century has focused much attention due to the severe consequences in the Sahel semi-arid region, which experienced a long period of drought in the 1970-80s (Folland et al. 1986; Giannini et al. 2003). It is broadly accepted that these changes were mainly driven by the sea surface temperature (SST) variability (Folland et al. 1986; Mohino et al. 2011; Rodríguez-Fonseca et al. 2015), amplified by land surface processes (Giannini et al. 2003; Kucharski et al. 2013). However, only a few works document the WAM variability prior to the 20th century (Nicholson et al. 2012; Gallego et al. 2015; Villamayor et al. 2018) due to the little information covering the 19th century and beyond. The paleo-archives are rare, often incomplete, and suffer from often poorly constrained chronologies. Moreover, these archives are rarely direct records of climate parameters, but indirect ones, namely historical, biological, or sedimentological. They integrate not only changes in environmental parameters but also

¹ Corresponding author : anne-marie.lezine@locean.ipsl.fr

45 the vital effect of species, the vulnerability or the resilience of ecosystems and the cultural
 46 adaptations of populations. Here we use pollen and other environmental proxies as well as
 47 historical chronicles to document the last millennium with a special focus on the period from
 48 1250 to 1850 CE including the transition between the Medieval Climate Anomaly (MCA; 950-
 49 1250CE) and the Little Ice Age (LIA; 1450-1850CE) periods characterised by global
 50 temperatures respectively above and below average (Nash et al. 2016; Villamayor et al. sub.).
 51 The aim of this **research** is not to record the climate variability at interannual scale but to
 52 discuss the timing, distribution and magnitude of the major secular environmental changes
 53 which punctuated the LIA in northern tropical Africa with a focus on the regional biomes and
 54 hydrological systems responses times to rainfall anomalies.

55 2. Material and method

56 2.1 Paleo-data

57
 58 This paper uses compilations of paleo-records from different sources with the highest
 59 available resolution (Table 1; Fig. 1). These data have the advantage of providing continuous
 60 records over the last millennium, but their temporal resolution is generally mostly
 61 (multi)decadal to centennial : pollen data are used for vegetation reconstructions (Elenga
 62 1992 ; Reynaud-Farrera et al. 1996; Ballouche 1998; Vincens et al. 1998; Salzmann et al. 2005;
 63 Ngomanda et al. 2007; Waller et al. 2007; Brncic et al. 2009; 2017; Lézine et al. 2011; 2013;
 64 2019; Lebamba et al. 2016; Tovar et al. 2019; Fofana et al. 2020; Catrain 2021), and
 65 micropaleontological, sedimentological and geochemical data to capture hydrological and
 66 climatic changes (Bertaux et al. 1998 ; Holmes et al. 1999 ; Street-Perrott et al. 2000 ; Schefuss
 67 et al. 2005 ; Wang et al., 2008 ; Shanahan et al. 2009 ; Mulitza et al. 2010 ; Nguetsop et al.
 68 2010 ; 2011 ; 2013 ; Carré et al. 2019 ; Lézine et al. 2019 ; Fofana et al. 2020 ; Catrain 2021).
 69 Compilations of historical chronicles (Nicholson 1978; 1980; 2013; Nicholson et al. 2012;
 70 Coquery-Vidrovitch 1997; Maley and Vernet 2013) and instrumental records (Gallego et al.
 71 2015) have also been examined, although the first are based on records of extreme events
 72 only (droughts, floods) and the second are limited in their temporal coverage. All these data
 73 are also scattered in a few limited areas of the Sahel (Senegal, Southern Mauritania, Niger
 74 River inner loop, Lake Chad basin) with possible redundancies.

75 The resulting data set is highly heterogeneous. Therefore, the data have been homogenized
 76 as follows: (1) only records covering the interval between 900 CE and present day with at least
 77 a 100-year temporal resolution have been taken into account, (2) in order to evaluate the
 78 relative amplitude of the environmental/climate change, we build a 6-point scale ranging from
 79 0, corresponding to the most arid environment (e.g., drying of lakes, salinization of water,
 80 increase of dust transport, opening of the vegetation cover) or the driest climate, up to 6,
 81 which refers to the most humid environment (e.g., high lake level, fresh water, dense
 82 vegetation cover) or the wettest climate. Decimal values were punctually added to identify
 83 minor changes in the paleoenvironment. This approach, based on our own expertise, provides
 84 a *qualitative* description of regional environmental and climatic conditions. It emphasises the
 85 major stages of environmental change while eliminating minor noisy variations (see
 86 supplementary Figure).

87

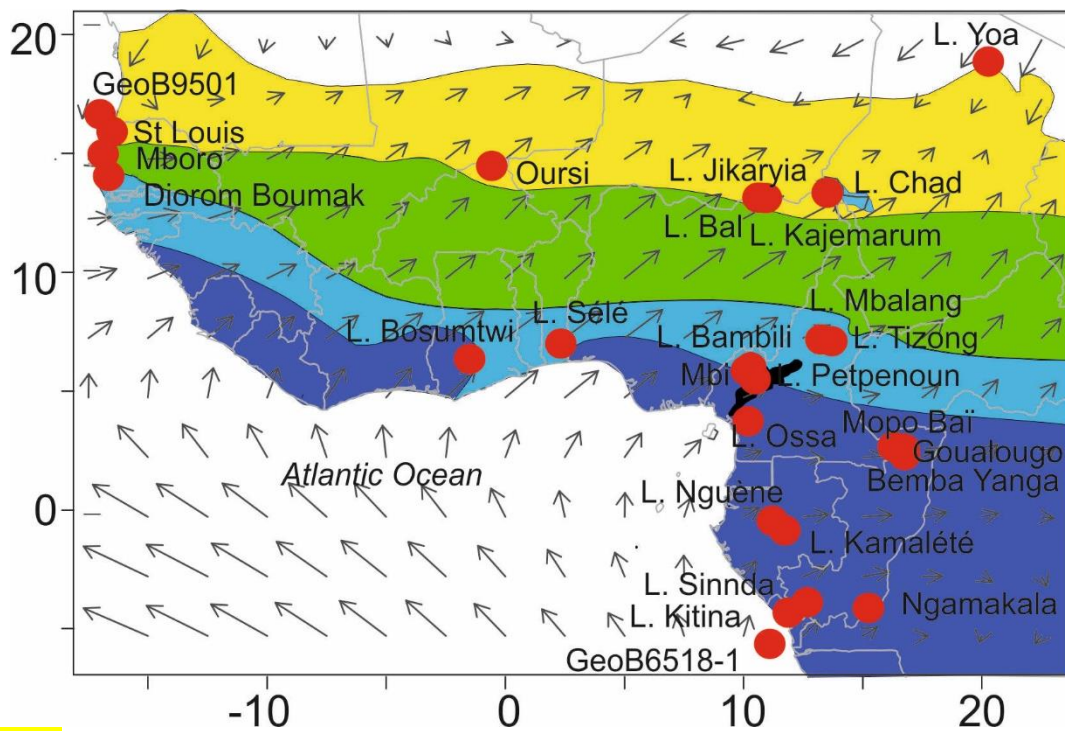
Site name	proxy	latitude	longitude	reference	Sector/vegetation zones
-----------	-------	----------	-----------	-----------	-------------------------

Lake Yoa	Pollen/sediment	19.057621	20.500690	Lézine et al. 2011	Sahara (Desert)
GeoB9501	Dust fraction	16.83333	-16.73333	Mulitza et al. 2010	Sahel
St Louis	Pollen/Diatom	16.03508	-16.48382	Fofana et al. 2020	Sahel (grasslands and wooded grasslands)
Mboro (Baobab)	Pollen/Diatom	15.149132	-16.909275	Lézine et al. 2019	Sahel (grasslands and wooded grasslands)
Oursi	Pollen	14.65283	-0.486	Ballouche 1998	Sahel (grasslands and wooded grasslands)
Dioron Boumak	Geochemistry	13.835809	-16.498372	Carré et al, 2019	Sahel/Savannah boundary
Lake Jikaryia	Sediment/Mineral-magnetic	13.313667	11.077	Waller et al. 2007; Wang et al. 2008	Sahel (grasslands and wooded grasslands)
Lake Bal	Ostracods/Chemistry	13.304	10.943	Holmes et al. 1999	Sahel (grasslands and wooded grasslands)
Lake Kajemaru m	Dust fraction/Geochemistry	13.303	11.024	Street-Perrott et al. 2000	Sahel (grasslands and wooded grasslands)
Lake Chad	Historical	13.053472	14.463469	Maley and Vernet 2013	Sahel (grasslands and wooded grasslands)
Lake Mbalang	Pollen/Diatoms	7.316	13.733	Vincens et al. 2000; Nguetsop et al. 2011	Savannah
Lake Tizong	Pollen/Diatoms	7.25	13.583	Nguetsop et al. 2013; Lebamba et al. 2016	Savannah
Lake Sélé	Pollen	7.15	2.433	Salzmann et al. 2005	Savannah
Lake Bosumtwi	Geochemistry	6.5	-1.416	Shanahan et al. 2009	Central Africa (lowlands) (Equatorial forests)
Mbi	Pollen	6.089273	10.348549	Lézine et al., in press	Central Africa (highlands)

					(Afromontane forests)
Lake Bambili	Pollen/ Geochemistry	5.936	10.242	Lézine et al. 2013	Central Africa (highlands) (Afromontane forests)
Lake Petpenoun	Pollen	5.64147	10.64531	Catrain 2021	Savannah
Lake Ossa	Pollen/Diatoms	3.800	10.75	Reynaud Farrera et al. 1996; Nguetsop et al. 2010	Central Africa (lowlands) (Equatorial forests)
Mopo Bai	Pollen/Geochemistry	2.240	16.261388	Brncic et al. 2009	Central Africa (lowlands) (Equatorial forests)
Bemba Yanga	Pollen	2.18726	16.52513	Tovar et al. 2019	Central Africa (lowlands) (Equatorial forests)
Goualougo	Pollen	2.0875	16.54722	Brncic et al. 2017	Central Africa (lowlands) (Equatorial forests)
Lake Nguène	Pollen	-0.2	10.466	Ngomanda et al. 2007	Central Africa (lowlands) (Equatorial forests)
Lake Kamalété	Pollen	-0.7166	11.7666	Ngomanda et al. 2007	Central Africa (lowlands) (Equatorial forests)
Lake Sinnda	Pollen/Sediment	-3.836111	12.8	Bertaux et al. 1996 ; Vincens et al. 1998	Central Africa (lowlands) (Equatorial forests)
Ngamakala	Pollen	-4.075	15.38333	Elenga 1992	Central Africa (lowlands) (Equatorial forests)
Lake Kitina	Pollen/Sediment	-4.27	12	Bertaux et al. 1996 ; Elenga et al. 1996	Central Africa (lowlands) (Equatorial forests)
GeoB6518-1	Alkenone / Geochemistry	-5.588333	11.221667	Schefuss et al. 2005	Central Africa

88
89
90
91

Table 1: Geographical positions, type and references of paleo-records used in this study (see Fig. 1).

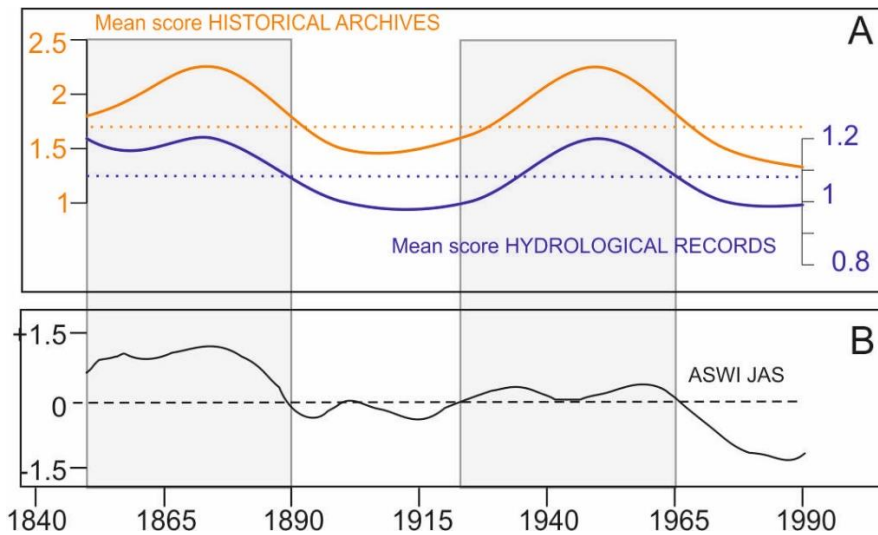


92
93 **Figure 1:** Map showing the location of paleorecords available in tropical West Africa
94 documenting the last millennium (Table 1). Grey arrows indicate the strength and direction
95 of the main 925 hPa monsoonal winds during boreal summer, i.e., the WAM rainy season
96 (NCEP-DOE AMIP-II Reanalysis (Kanamitsu et al., 2002)). In color, vegetation units from White
97 (1983): dark blue: Guineo-Congolian rainforest; light blue: Sudano-Guinean woodland and
98 wooded grassland (here referred to as Savannah (vegetation) zone); green: Sudanian
99 woodland and wooded grassland; yellow: Sahelian grassland and wooded grassland. black:
100 Afromontane forest.

101
102 In order to verify whether the methodology employed provides reliable indications of
103 environmental change for the period prior to the instrumental records scores of the WAM
104 rainy season (July to September), multidecadal hydrological changes from natural archives and
105 historical data (Table 1) in the Sahel are compared to the African Southwesterly Index (ASWI)
106 developed by Gallego et al. (2015) over 1840-1990 CE. The ASWI is based on JAS wind direction
107 data (i.e the persistence of the low-level southwesterly winds) from historical measurements
108 available since 1839 in a region over the Atlantic, close to West Africa (29°W–17°W, 7°N–
109 13°N). The ASWI is strongly correlated with the observed Sahel precipitation since 1900 and
110 is, therefore, presented as a good indicator of its variability. It was validated against
111 instrumental observations as a good measure of WAM intensity during the rainy season over
112 the instrumental period (Gallego et al. 2015). Positive values of the ASWI indicate periods
113 when the monsoon is well established over the Sahel, and thus define periods of heavy rainfall
114 in the region, which is consistent with observational data (Descroix et al., 2015). Figure 2
115 shows strong similarities between our historical records and the ASWI. However, historical
116 records give a slightly different magnitude of dry and wet anomalies that reflects the
117 sensitivity of populations to periods of drought or flooding. Our assessment of hydrological

118 conditions based on natural archives reflects historical records variations but with a somewhat
 119 weaker magnitude. This is probably due to the much lower temporal resolution of the
 120 available data (25-50 yrs on average). It is also worth noting that the lake data corresponds
 121 to a precipitation/evaporation balance and not the precipitation amounts at a given site.
 122 Nevertheless, the curves are remarkably similar and point to wet periods centred ca 1875 and
 123 1950 CE.

124



125
126

127 **Figure 2:** Observed and reconstructed rainfall anomalies over the Sahel during the 1840-1990
 128 CE period. (A) the mean scores from historical (yellow curve) and natural archives (blue curve)
 129 for the Sahel (Nicholson, 1978; 1980; Nicholson et al. 2012; 2013; Coquery-Vidrovitch, 1997;
 130 Holmes et al., 1999; Street-Perrott et al. 2000; Waller et al. 2007; Wang et al. 2008; Mulitza et
 131 al. 2010; Maley and Vernet, 2013; Lézine et al. 2019). The dotted yellow and blue lines
 132 correspond respectively to the historical and paleohydrological archives mean scores during
 133 the period 1850-1990CE. They allow identifying anomalously wet and dry periods. (B) The
 134 African Southwesterly Index (ASWI) developed by Gallego et al. (2015) as a measure of rainfall
 135 anomalies in Sahel during the WAM rainy season (July to September).

136

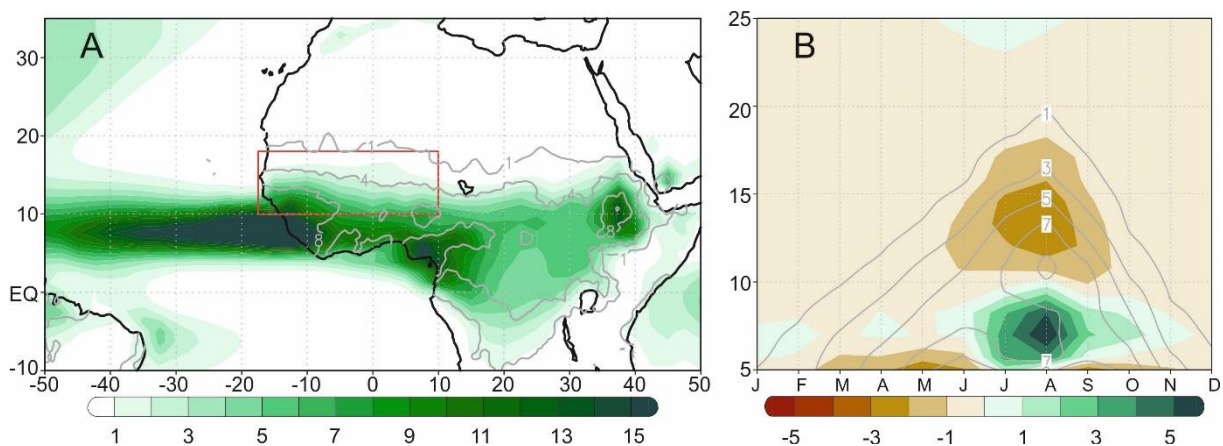
137 2.2 Model experiments

138 In this study we compare reconstructed environmental changes in Western Africa to those
 139 simulated in the past1000 model experiment covering the 850-1850 CE climate performed as
 140 part of 4th phase of the Paleoclimate Modelling Intercomparison Project (PMIP4; Jungclaus et
 141 al. 2017; Kageyama et al. 2017) by the IPSL-CM6A-LR model version developed for the Coupled
 142 Model Intercomparison Project phase 6 (CMIP6) at Institut Pierre-Simon Laplace (Boucher et
 143 al. 2020; Lurton et al. 2020). The IPSL-CM6A-LR model couples the atmospheric component
 144 LMDZ (Hourdin et al. 2020) to the land surface model ORCHIDEE (d'Orgeval et al., 2008) and
 145 to the ocean model NEMO, which includes other models to represent sea-ice interactions
 146 (Rousset et al., 2015) and biogeochemistry processes (Aumont et al. 2015). The atmospheric
 147 and land-surface grid have a resolution of 2.5° in longitude and 1.3° in latitude with 79 vertical
 148 layers. The oceanic component has 75 vertical levels with a mean spatial horizontal resolution
 149 of about 1° and a refinement of 1/3° near the equator. This model reproduces fairly well the
 150 ENSO (McPhaden et al. 2006) seasonality despite the sea surface temperature anomalies
 151 extending too westward in the central Pacific during El Niño events. The spatial pattern of the

152 Atlantic Multidecadal Variability (AMV, Deser et al. 2010) teleconnection in the Pacific is
 153 consistent with observations but the tropical Atlantic variability is relatively weaker. Unlike
 154 most current state-of-the-art CMIP6 models, the IPSL-CM6A-LR model simulates a
 155 predominant secular variability in the Atlantic with AMV peaks separated by about 200 years
 156 (Boucher et al., 2020).

157 The past1000 IPSL-CM6A-LR model experiment is designed to simulate the climate response
 158 to natural forcings recommended by PMIP4 (Jungclaus et al. 2017) and covering the pre-
 159 industrial millennium (850-1849CE), namely the time varying astronomical parameters, the
 160 trace gases (Meinshausen et al. 2017; Matthes et al. 2017), the eVolv2k volcanic forcing
 161 (Toohey and Sigl 2017), the SATIRE-M 14C solar activity with an adaptation of the spectral
 162 irradiance to the CMIP6 *historical* forcing and the land use forcing (Lawrence et al. 2016).
 163 Three past1000 IPSL-CM6A-LR model simulations have been performed and branched off from
 164 various initial conditions in a 600 years long spinup run with fixed external radiative forcing to
 165 the year 850 CE. This spinup run, itself branched off from the IPSL-CM6A-LR pre-industrial
 166 control (piControl) run with constant external radiative forcing, has been performed to avoid
 167 any spurious drift in the past 1000 experiments that could be related to the adjustment of the
 168 slow components of the climate system (such as the ocean), to the different radiative balance
 169 at the beginning of the last millennium as compared to the pre-industrial levels.

170
 171



172
 173

174 **Figure 3:** Climatological bias of simulated monthly precipitation. A) JAS mean averaged across
 175 (colors) the 2000-year piControl run and (contours) the 1891-2019 period in GPCPv2020
 176 observational database. B) (colors) Meridional seasonal cycle of the 10° W – 10° E mean model
 177 bias (simulation minus observations) compared to (contours) the GPCPv2020 climatology. All
 178 units are mm/day. Red box in (A) indicates the Sahel region (17.5°W-10°E; 10°-18°N).

179

180 The IPSL-CM6A-LR model reproduces the observed climatological distribution of maximum
 181 rainfall across West Africa during the WAM rainy season (Fig. 3A). The timing of the simulated
 182 WAM seasonal cycle is also in good agreement with observations, with a well-defined onset
 183 of the rainy season in July and then a demise after September (Fig. 3B). However, the
 184 northward shift of maximum rainfall over the Sahel during the rainy season is underestimated
 185 by the model by about 4° (the model's maximum in August is ~7°N and the observed one at
 186 11°N). As a result the climatological rain belt over West Africa is slightly more constrained to
 187 tropical regions compared to observations and dryer Sahel on average. However, the well-

188 characterized WAM seasonal timing suggests that there are no remarkable biases affecting
189 the simulated precipitation variability.

190 Then, to characterize the simulated Sahel rainfall multidecadal variability over the past
191 millennium and contrast to the reconstructed environmental series, an index is calculated as
192 the 10-year low-pass-filtered Sahel precipitation anomalies in the rainy season from past1000
193 simulations. Seasonal precipitation anomalies from July to September (JAS), relatives to the
194 piControl climatology, are area-weighted and averaged across the Sahel region (red box in Fig.
195 3A), then filtered with a 10-year centered moving mean with truncated endpoints (i.e., only
196 averaging existing elements within the 10-year window). An ensemble-mean index is also
197 performed to highlight the forced component of the Sahel multidecadal variability in response
198 to natural forcings that are common to the three past1000 members, such as the effect of
199 large volcanic eruptions, in contrast to the internal variability.

200

201 3. Results

202 3.1 The hydrological records

203

204 The hydrological records provide a contrasting picture from one region to another: the Sahel,
205 the Sudano-Guinean Savannah zone and the tropical forests. They also reveal some local
206 exceptions. As already noted (e.g., Vincens et al. 1999), the local hydrogeological context may
207 strongly affect the individual response of lakes and wetlands to rainfall variations and partly
208 explains this apparent heterogeneity.

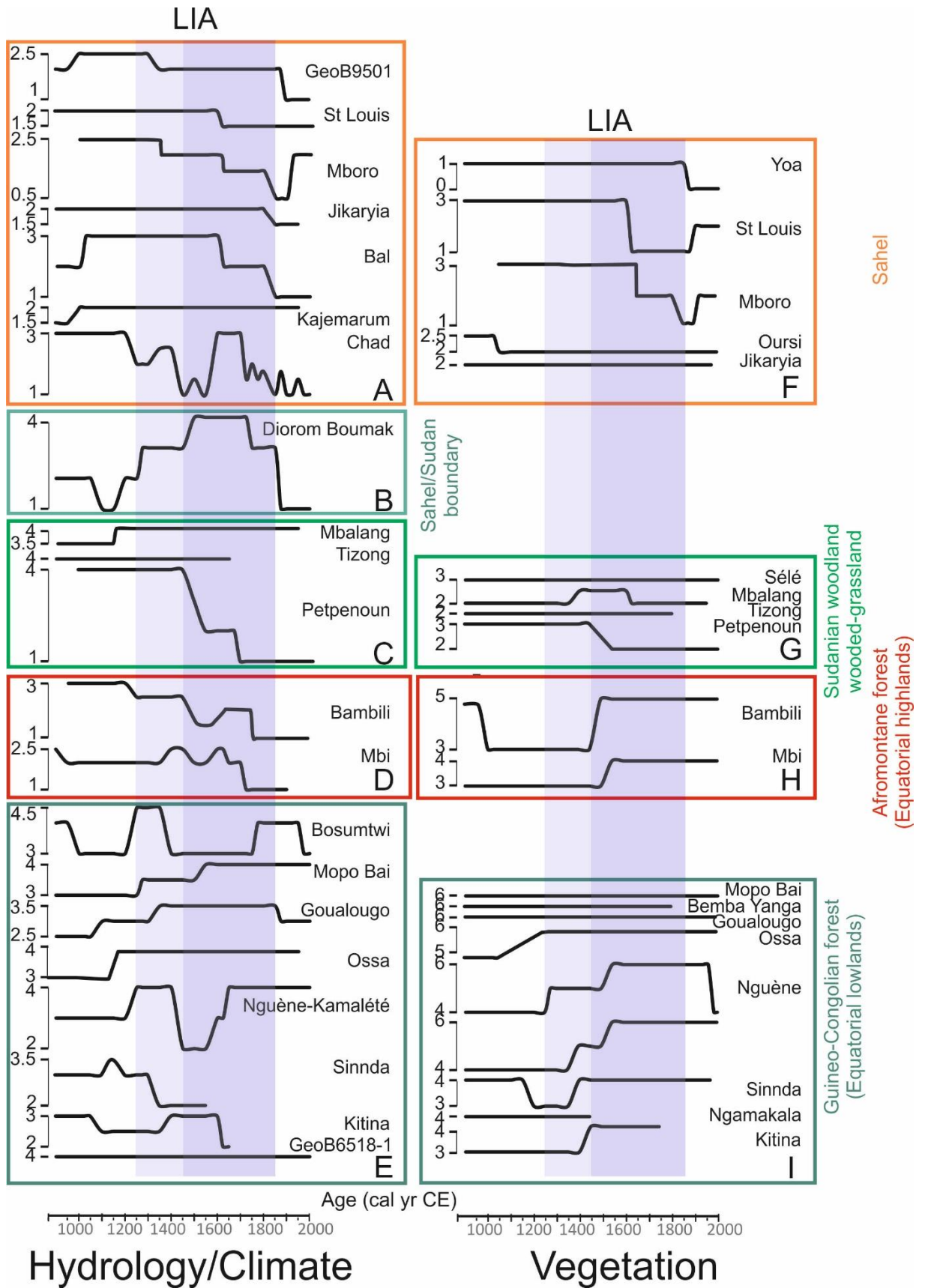
209 The main characteristics of the hydrological evolution in the Sahel, in the Savannah zone and
210 in low- and high-altitude equatorial forests can be summarized as follows (Fig. 4):

211 • Data from the central and western Sahel (Fig. 4A) point to a relatively dry period at the
212 end of the first millennium (900CE) at Bal, Kajemarum and in the Senegal River
213 watershed (GeoB9501). A wet period followed, already present at Mboro near the
214 littoral, which lasted up to 1350CE. Except at Kajemarum and Jikarya, where
215 hydrological conditions remained relatively stable, a gradual trend toward increased
216 aridity is recorded in two steps dated ca. 1625CE and 1800CE, respectively. Then,
217 during the last two centuries, only minor fluctuations occurred in a general context of
218 widespread aridity.

219 In the lake Chad area, Maley and Vernet (2013) depict a rather different and complex
220 history probably due to the variety of the archives they used (both historical and
221 natural) and also to the complexity of the hydrology of this immense water body
222 (Pham-Duc et al. 2020) fed by underground waters and by rivers of distant
223 geographical origin. The authors identify two major periods of flooding in the lake
224 Chad area: from the onset of the millennium to ca. 1200CE, then between 1600 and
225 1700CE, with a series of dry periods in between then from 1700CE onwards.

226 • Only three sites document the hydrological evolution of the Savannah zone south of
227 the Sahel (Fig. 4C). These sites are located in the centre of the savannah zone (White
228 1985): two crater lakes on the Adamawa plateaus (Mbalang and Tizong) and the other
229 at the mouth of the tributary of Lake Petpenoun in the Grassfields region of Cameroon.
230 The Adamawa lakes do not show any significant hydrological changes throughout the
231 last millennium. In contrast Petpenoun records a clear evolution towards aridity which
232 started ca. 1425CE and culminated ca. 1650CE up to the present day.

- 233
- 234
- 235
- 236
- 237
- 238
- 239
- 240
- 241
- 242
- 243
- 244
- 245
- 246
- 247
- 248
- 249
- 250
- 251
- 252
- 253
- 254
- Diorom Boumak (Fig. 4B) is situated at the southern boundary of the Sahel, in the littoral mangrove of the Saloum estuary. In contrast to the other sites from the Sahel and savannah zone this site records a remarkable wet period between 1500CE and 1800CE. As elsewhere however, aridification started ca. 1800CE.
 - The equatorial lowlands is characterized by contrasting hydrological situations reflecting the diversity of local hydrogeological settings (Fig. 4E). Low lake levels are recorded at Bosumtwi, Mopo Bai, Goualougo, Nguène-Kamalété and Ossa during a period centred around 1100CE in contrast to Sinnda and Kitina where moist conditions occurred. Moisture increased as soon as 1350CE at Goualougo and continued up to 1400CE at Mopo Bai and Kitina. Then, there is a clear opposition between Sinnda, Nguène-Kamalété and Bosumtwi where low lake levels occurred during a dry phase between ca 1350 and 1700CE and Mopo Bai, Goualougo, Ossa and Kitina, which are characterized by wetter conditions. In any case, the marine record at the mouth of the Congo River (GeoB6518-1) suggests that all these hydrological variations in the equatorial lowlands remained of relatively low amplitude.
 - In the Cameroon highlands (Fig. 4D), hydrological conditions steadily declined as shown at lake Bambili, starting from ca. 1250 and culminating ca. 1675CE. This gradual trend is interrupted ca. 1500CE by a more pronounced phase of lake level lowering. The Mbi swamp displays a rather different pattern: here, the water level was relatively low throughout the whole last millennium except to two discrete wetter phases ca. 1450 and 1650CE.



255
256
257
258
259

Figure 4: Mean scores of hydrological and vegetation changes along a North-South transect from the northern limit of the Sahel (Yoa) to the Congo basin (GeoB6518-1). Data are grouped within the phytogeographical entities defined by White (1983) in tropical Africa: Sahelian

260 grassland and wooded grassland, Sudano-Guinean savannah, highland Afromontane forest,
 261 lowland Guineo-Congolian forest. The shaded vertical bands indicate the transition period
 262 between the medieval climate anomaly and the Little Ice Age (1250-1450CE light shading) and
 263 the LIA (1450-1850CE dark shading).

264

265 3.2 Pollen data

266

- 267 • In the open landscapes of the Sahara, Sahel and Savannah zones, vegetation changes
 268 were of minor amplitude except at sites where gallery forests were previously well
 269 developed. It is in the westernmost part of the Sahel that the most profound changes
 270 in vegetation cover are recorded : In the Niaye area (Mboro) and in the Senegal river
 271 delta (St Louis), the degradation of the landscape originated ca. 1300CE and
 272 accelerated ca. 1600CE to a maximum reached ca. 1850CE (Fig. 4F). A discrete
 273 vegetation recovery is then recorded in the 19th century. In contrast, sites from the
 274 central Sahel (Oursi and Jikaryia) remained relatively stable throughout the last
 275 millennium in spite of a slight degradation recorded at Oursi ca. 1050CE. North of the
 276 Sahel (Yoa), the aridification of the desert landscape accelerated from the 19th century
 277 onward. South of the Sahel, in the Savannah zone, lakes Tizong and Sélé do not record
 278 any marked environmental change contrary to Petpenoun where a slight degradation
 279 is recorded ca. 1425CE (Fig. 4G). At Mbalang, a discrete phase of vegetation recovery
 280 occurred between ca 1400-1600CE.
- 281 • The forest cover remained roughly unchanged in the central forest massif (Mopo Baï,
 282 Bamba Yanga, Goulalougo, Fig. 4I). In the western regions by contrast, (Ngamakala,
 283 Kitina, Lac Ossa, Nguène and Kamalété the forest gradually developed since 1250-
 284 1350CE in spite of the discrete hydrological fluctuations. In the Cameroon highlands
 285 (Fig. 4H), the forest development occurred later, ca 1550-1500CE, after a phase of
 286 forest clearance from 1000 to 1450CE.

287

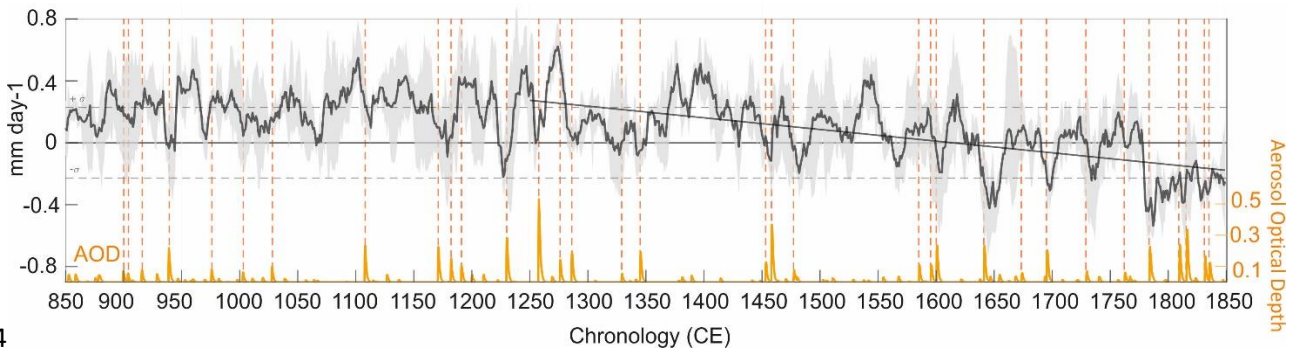
288 3.3 Model results

289

290 The index of the ensemble-mean Sahel JAS precipitation simulated over the past millennium
 291 reveals a change from a relatively wet mean state in the MCA (950-1249 CE) to a drier one in
 292 the LIA (1450-1849) (Fig. 5), suggesting a shift of the average WAM rainfall regime. Such
 293 continuous decline presents a linear rate of the seasonal Sahel rainfall of -0.7 mm per decade
 294 over 1250-1849CE, resulting in a 7% loss of the mean precipitation in the LIA relative to MCA
 295 (Fig. 5). Regarding decadal variations, the ensemble-mean index of past1000 Sahel
 296 precipitation almost doubles its variability in the LIA with respect to the MCA (the variance in
 297 859-1249CE is 51% higher than in 1450-1849CE), which suggests a more unstable rainfall
 298 regime, apart from drier on average, by the late past millennium in response to natural
 299 external forcings. As shown by Villamayor et al. (2022), such a simulated long-term drying
 300 trend and increased LIA Sahel precipitation decadal variability is related to the volcanic forcing
 301 influence on SSTs, which integrates the induced radiative cooling (Fang et al. 2021). The more
 302 frequent large volcanic eruptions during the LIA, as compared to the MCA, is integrated by the
 303 ocean long memory, leading to a gradual SST decrease that is more pronounced in the
 304 Northern Hemisphere than the Southern Hemisphere. The relative North Atlantic SST cooling
 305 trend along 850-1849CE, gradually promotes a southward shift of the Inter-Tropical
 306 Convergence Zone (ITCZ) and a weakening of monsoon moisture inflow to Western Africa. The

307 long term WAM weakening is further amplified in the few years following any new large
 308 volcanic event, which occurrences are indicated by the vertical dotted lines on Figure 5. As a
 309 consequence, more frequent negative rainfall anomalies lasting at least 5 consecutive years
 310 are also evident during the LIA as compared to the MCA, with significant drying that can persist
 311 up to 60 years around clusters of eruptions such as those of the 19th century.

312
 313



314
 315

Figure 5: Multidecadal Sahel rainfall variability in IPSL-CM6A-LR past1000 simulations. Black line: 10-years low pass filtered index of Sahel JAS precipitation anomalies averaged in boxed area in Figure 3 (i.e., 10°-18°N and 17.5°W-10°E). The black line corresponds to the ensemble mean, the grey shading to the ensemble spread and diagonal line to the 1250-1849 CE linear fit. Dashed horizontal lines show the +/- standard deviation of the equivalent piControl index. The volcanic forcing used in the IPSL-CM6A-LR model experiments is shown by the orange curve as the globally averaged Aerosol Optical Depth (AOD). Red vertical dotted lines indicate the occurrence of strong volcanic eruptions about the size or larger than the Pinatubo eruption (June 1991) defined when the tropical (20°S-20°N) or northern extratropical (50°N-90°N) mean AOD is larger than 0.1.

326

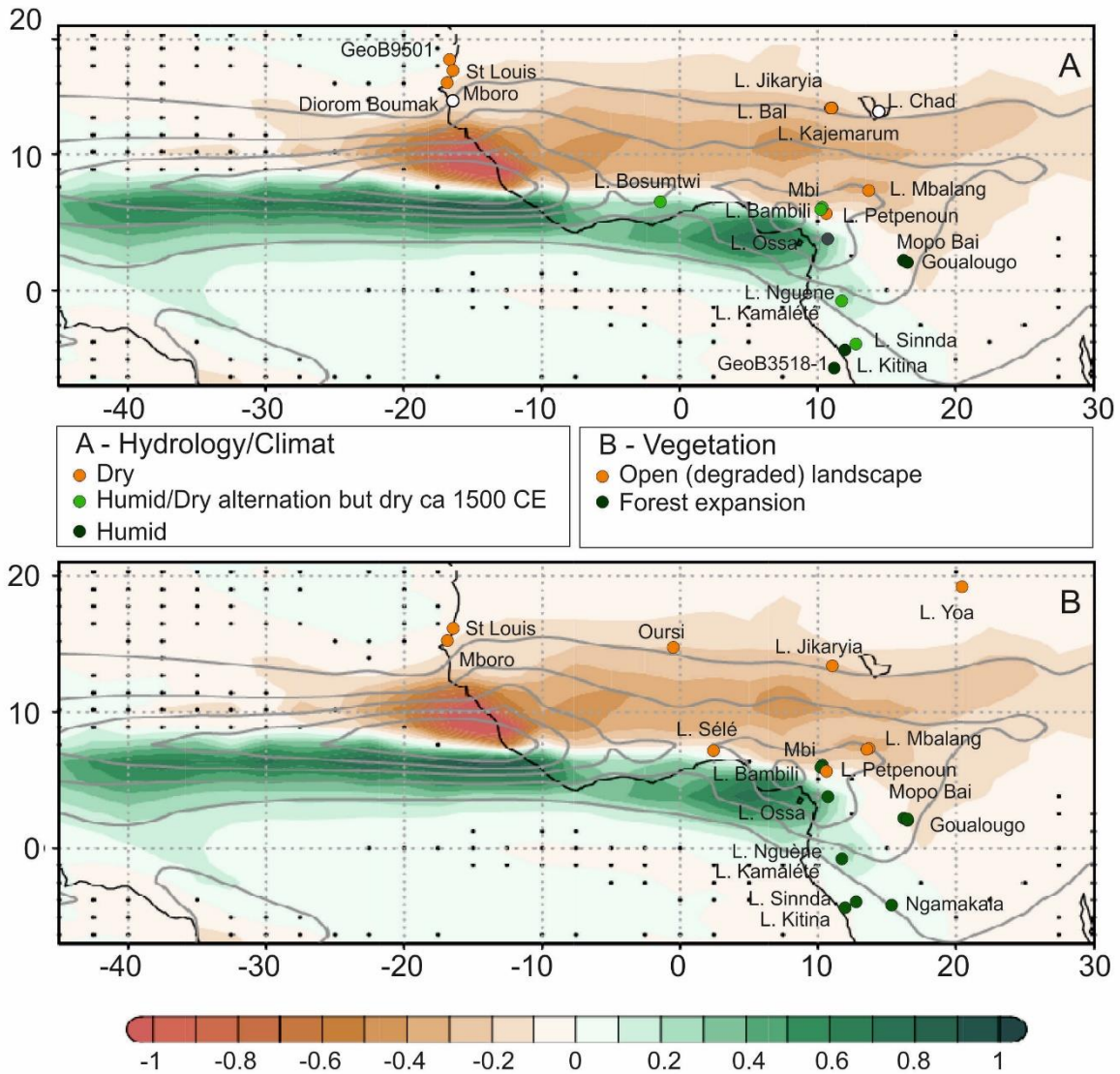
327 4. Discussion

328

329 4.1 Hydrology and Climate changes at secular timescale

330

331 Data and past1000 model simulations show a strong North-South contrast between the Sahel
 332 and Savannah zones, both subjected to severe drying during the LIA, and the equatorial areas,
 333 spanning the Gulf of Guinea coast, suggesting an overall change of the WAM.



334
335

336 **Figure 6:** Distribution of JAS rainfall anomalies difference between the LIA (1450-1849 CE) and
 337 the MCA (950-1249 CE) as simulated by the IPSL-CM6A-LR model in the past1000 ensemble-
 338 mean (shading, mm day⁻¹) compared to hydrological/dust (A) and vegetation (B) paleorecords
 339 during the LIA shown as dots following the same color scale as simulated anomalies. Grey
 340 contours indicate the piControl climatology from 2 mm day⁻¹ in intervals of 4 mm day⁻¹.
 341 Stippling indicates disagreement across the three past1000 members on the sign of the
 342 represented difference.

343

344 The difference between the simulated past1000 JAS precipitation during the LIA and the MCA
 345 shows a characteristic distribution of a weakened WAM associated with a southward shift of
 346 the ITCZ, with less rainfall across the Sahel and more in the Gulf of Guinea coast (Fig. 6). These
 347 simulated anomalies are consistent with the overall distribution of hydrological and
 348 vegetation proxy reconstructions.

349

350 4.1.1 Hydrology

351

352 Three major regions can be recognized from the paleohydrological records: The Sahel and
353 Savannah zones, with drying trend; the center of the Congo Basin, which exhibit an opposite
354 trend of increasing humidity; and the boundary between the dry and humid domains defined
355 by the equatorial sectors closest to the coast or in mountain, where an alternation of wet and
356 dry phases is recorded. Two paleo-records differ from this general picture: that of Lake Chad,
357 where a period of flooding is recorded ca 1600CE, and that of the Diorom Boumak, where the
358 LIA is entirely characterized by a wet period (Fig. 4). As evoked above, the multiple origins of
359 the data and the complex hydrological system of Lake Chad may have introduced a bias into
360 the hydrological record and may explain (at least partly) the difference with the other Sahelian
361 archives. It is also likely that the rivers that feed the lake, which originate from southern
362 regions (the Chari and Logone rivers and their tributaries), may have caused an influx of water
363 during the short humid phase recorded on the Cameroon highlands (Bambili and Mbi) ca
364 1600CE. The case of the Diorom Boumak site is more complex: the historical records
365 mentioned by Maley and Vernet (2013) or Carré et al. (2019), among others, indicate that the
366 Saloum sector was wetter than the rest of the Sahel during part of the 16th century, allowing
367 for the establishment of two harvests per year. This may have been due, according to Maley
368 and Vernet (2013), to the occurrence of two rainy seasons, one in the core of the WAM season
369 in summer and another (usually of lesser importance) referred as “Heug rains” linked to polair
370 air intrusions in winter (Le Borgne 1979).

371

372 4.1.2 Vegetation

373

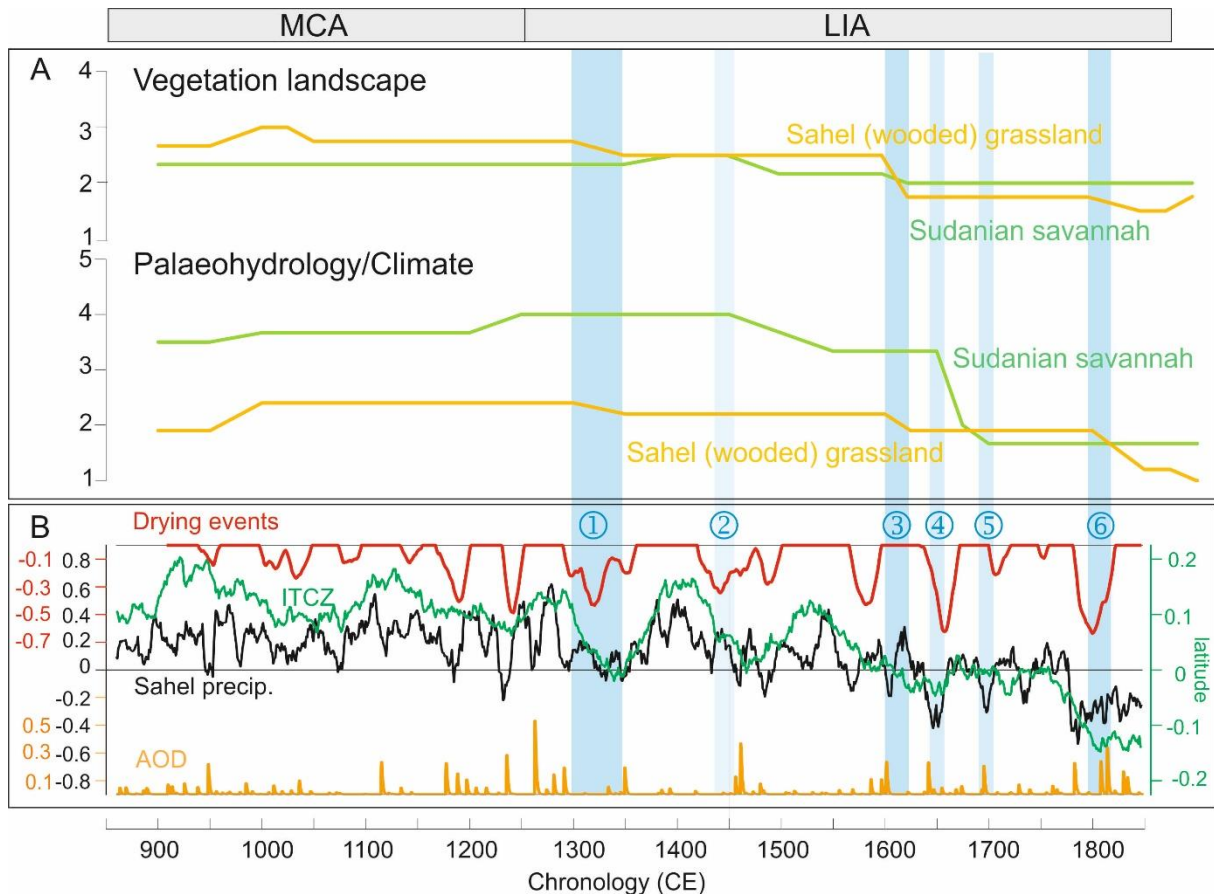
374 In the central Sahel, already degraded prior to the LIA (Lézine 2021), such as at Oursi, no
375 significant change occurred in the vegetation landscape which remained open throughout the
376 last millennium (Fig. 4B). The same pattern is observed in the wettest areas of the Congo Basin,
377 where the forests remained unchanged in composition and physiognomy (Tovar et al. 2019).
378 Elsewhere in the forest galleries of the Sahel and the Savannah zone (Mboro, St. Louis,
379 Petpenoun) the evolution of vegetation mirrored that of hydrological conditions while
380 recording a gradual degradation that culminated around 1800-1850 CE. In the westernmost
381 sector of the Sahel (Mboro, St Louis), the data suggest however a slight recovery of the
382 vegetation cover during the last few decades.

383 In contrast, both high and low elevation sites from the equatorial forest regions show an
384 opposite trend with marked forest recovery that began in the early years of the LIA and
385 accelerated around 1450CE. The forest expanded in the Equatorial lowlands despite increased
386 human presence has already been noted by Vincens et al. (1999). That means that the local
387 hydrological variations, and particularly the 1500 CE dry event, were of too small an amplitude
388 to impact forest dynamics. At most, a plateau in forest recovery is observed at that time
389 (Nguène, Kamalété). While the forest recovery was gradual at low altitudes, it seems to have
390 occurred more abruptly in the highlands.

391

392 4.2 The chronology of events at multidecadal timescale: focus on the Sahel and Savannah 393 zone

394



395
 396 **Figure 7:** Multiproxy records of hydrology and vegetation during the last millennium in the
 397 driest biomes (Sahel and Savannah zone) in western Africa (A) and long-term evolution of
 398 rainfall over the Sahel as simulated by the IPSL-CM6A-LR past1000 model (B). Panel B: (Black
 399 line) 10-year filtered ensemble-mean Sahel precipitation index (mm day^{-1}). (Green line) 50-
 400 year filtered anomalous latitudinal position of the JAS ITCZ (defined as the latitudinal
 401 maximum zonal-mean rainfall in 40°W - 10°E) in the past1000 simulations respectively to the
 402 piControl JAS mean position (in degrees of latitude). (Orange line) Global-mean AOD (volcanic
 403 forcing). (Red line) Sahel Drying Persistence Index defined as the 50-year running negative
 404 trend values over the Sahel ensemble-mean JAS precipitation index (mm day^{-1} per 50 years).
 405 Blue bars and numbers highlight the main climate/environmental degradation thresholds
 406 identified in the paleo-records.

407

408 Environmental changes in the Sahel and Savannah zones during the LIA occurred in the context
 409 of widespread environmental degradation that followed the severe environmental crisis at
 410 the end of the African Humid Period (AHP; deMenocal et al., 2000). Between 3300 and 2500
 411 cal yr BP (Lézine, 2021), the forests and woodlands, that widely expanded across the plains
 412 and mountains of West Africa, strongly declined. This is particularly striking along the Atlantic
 413 coast of Senegal, between 15° and 17° N where specific environmental conditions related to
 414 the proximity of the sea and the presence of a water table near the surface favored the
 415 development of exceptionally dense forest galleries of humid tropical affinity during the AHP
 416 (Lézine 1989). As a result of this major environmental crisis, the Sahel and Savannah zone took
 417 on its modern aspect of semi-desert grassland and wooded grassland. In this context,
 418 discernible environmental fluctuations, particularly in vegetation, are of limited magnitude,
 419 with the exception of sectors where forest galleries were widely established during the AHP.

420

421 To discuss the chronology of events that punctuated the LIA, paleo-data were averaged in
 422 each geographical area (Sahel, Savannah zone) in the two categories covered by our study:
 423 hydrology/climate and vegetation (Fig. 7A). A Drying Persistence Index was constructed from
 424 our model results in order to quantify the Sahel precipitation deficit over at least 50-year
 425 periods (red curve in Fig. 7B). It is defined at each year as the negative linear trend of the Sahel
 426 ensemble-mean JAS precipitation (black curve in Fig. 7B) across the 50 previous years. We use
 427 50 years to be consistent with the multi-decadal to centennial temporal resolution of the
 428 paleo-data.

429 The past1000 simulations represent several drying events of various amplitude and duration
 430 during the MCA that do not correspond to any major change in the vegetation of the Sahel
 431 and Savannah zone. Instead, the environment in these two areas appears to be characterized
 432 by a relatively stable humid regime (Fig. 7A). This is coherent with the rainy mean state
 433 represented by the past1000 simulations over the MCA, which is associated with an
 434 anomalous northward ITCZ position (green curve in Fig. 7B) all over this period compared to
 435 the LIA.

436 At the end of the MCA, two early warning signals (Lenton 2011) of Sahel drying events centred
 437 at 1170 and 1240 CE are identified in our model experiments. The intensity and brevity of
 438 these two events contrast with the minor dry phases identified prior to the LIA since the onset
 439 of the last millennium. The Drying Persistence Index at these two events, which timing
 440 coincides with the occurrence of large clusters of volcanic eruptions (orange curve Fig. 7B),
 441 reaches over -0.3 mm day^{-1} across 50 years. Both events preceded the onset of the LIA gradual
 442 drying trend starting at 1250CE. This drying trend was sustained by the southward migration
 443 of the ITCZ which shifts south of the piControl mean position at 1600 CE. It is consistent with
 444 the continuous degradation of hydrological and vegetation conditions since 1250 CE in the
 445 Sahel and Savannah zone identified in our multi-proxy records.

446 Several abrupt drying events larger than those identified during the MCA punctuated the LIA,
 447 some of which reaching over -0.5 mm day^{-1} across 50 years. Despite the difference in temporal
 448 scale between the two approaches used here, there is a striking agreement between the major
 449 simulated droughts and the environmental degradation steps in our paleorecords (blue bars
 450 in Fig. 7). These degradation periods, in turn, span the largest eruptions from ca. 1250 to ca.
 451 1850CE, which are associated with the multi-decadal variability of Sahel precipitation over the
 452 past millennium in PMIP4 multi-model experiments (Villamayor et al. sub.).

453 **4.2.1 Steps in the degradation of the climate and the environment in the Sahel**

454 Three major steps are identified:

- 455 - The first dramatic environmental degradation occurred between 1290 and 1350 CE
 456 (event 1), i.e., ca. 50 years after the first warning signal and lasted about 60 years. Dust
 457 fluxes to the ocean, which had stabilized during the medieval warm period, increased
 458 (Mulitza et al. 2010) whereas lake levels dropped in the interdunal depressions in the
 459 western Sahel leading to the salinization of the waters (Lézine et al. 2019).
- 460 - The second stage in the degradation of environmental conditions occurred ca 1600CE
 461 (event 3). The environmental degradation was common to the entire Sahel (Bal,

462 Mboro, St Louis) while corresponding to a major collapse of the forest galleries at
 463 Mboro. Here also, a time lag of ca. 50 years can be observed between the onset of a
 464 drought phase and the response of the vegetation.

465 - The ultimate environmental threshold is recorded ca 1800CE (event 6). It resulted in
 466 the widespread lowering of lake levels, the massive contribution of dust to the ocean,
 467 and the irreversible destruction of forest galleries in the western Sahel in response to
 468 an abrupt drop in rainfall ca 1800CE, already observed by Carré et al. (2019) in the
 469 Saloum river delta. By accounting for a catastrophic decrease in precipitation of -0.6
 470 mm day^{-1} over 50 years in our model experiments, this climatic tipping point related
 471 to closely spaced large volcanic eruptions (starting with Laki eruption in 1783 CE
 472 followed by the eruptions cluster over the 1809-1835 CE period including the 1815
 473 Tambora event), at the origin of the modern environmental conditions in the Sahel,
 474 was twice as large as the early warning signals identified at the end of the MCA.

475 Our data-model comparison suggests that there was a time lag of several decades (typically
 476 50 years) between the climate signal and the environmental response. If this time lag is highly
 477 probable, its duration and origin require further investigation. It may indeed result from the
 478 resilience of plants to climate change but we cannot exclude the memory effect of aquifers
 479 already observed by Aguiar et al. (2010) that may induce a delay between the climate signal
 480 and its effects on ecosystems. The uncertainty associated with the ages, whether it comes
 481 from the data or from the modelling, can also play a role by increasing or reducing this
 482 response time.

483 **4.2.2 The Savannah zone:**

484
 485
 486 As the ITCZ moved to more southerly latitudes, some of the drought events reconstructed in
 487 the Sahel had a major impact in the Savannah zone. Here, data is particularly sparse and, as in
 488 the Sahel, changes in vegetation are hardly distinguishable in these already highly degraded
 489 environments, such as at Lake Sélé (Salzmann et al. 2005). It is at Lake Petpenoun (Catrain
 490 2021) that the evidence is the clearest due to the presence of a gallery forest and pronounced
 491 hydrological changes at the core site.

492 We find that the last step of degradation of the savannah vegetation occurred during event 3
 493 also observed in the Sahel. Events 2 (1447-1493CE), 4 (1643-1657CE) and 5 (1691-1707CE)
 494 correspond only to phases of hydrological degradation that are not reflected in the regional
 495 vegetation. Data are still too rare to generalize this observation to the entire Savannah zone
 496 and could only account for local conditions.

497 **5. Conclusion**

498
 499
 500 Despite the uncertainties associated with data scarcity and heterogeneity, our study shows a
 501 remarkable agreement between the data and our past1000 model experiments for
 502 reconstructing the climate and environmental changes in response to natural forcing that
 503 characterized the LIA in western Africa. It highlights a North-South contrast between the
 504 dryness of the Sahel and the humidity of the equatorial zone. Despite the major difficulty
 505 related to the type of vegetation at play in the Sahel and the Savannah zone already degraded
 506 since the end of the AHP, major steps in the degradation of the environment can be identified.
 507 Our most remarkable results consists in (1) the identification of two early warning signals at

508 1170 and 1240CE, i.e. prior to the progressive LIA drying of the Sahel that lead to the climatic
 509 tipping point at 1800-1850CE. This tipping point marks the setting of arid conditions (the driest
 510 condition since 850CE) which still persist today; (2) the identification of abrupt drought events
 511 which punctuated the LIA, the most important of them has impacted both the Sahel and the
 512 Savannah zone ca. 1600CE. The consistency between proxy records and our model
 513 experiments suggests a strong role of large volcanic eruptions in shaping Sahel environmental
 514 changes over the pre-industrial millennium. Further work relying on large ensembles of
 515 climate and vegetation models will help assess such hypothesis.

516

517 **Code availability**

518

519 The IPSL-CM6A-LR model code used in this work was frozen (version 6.1.0) and subsequently
 520 altered only for correcting diagnostics or allowing further options and configurations. Versions
 521 6.1.0 to 6.1.11 are therefore bit-reproducible for a given domain decomposition, compiling
 522 options and supercomputer. LMDZ, XIOS, NEMO and ORCHIDEE are released under the terms
 523 of the CeCILL licence. OASIS-MCT is released under the terms of the Lesser GNU General Public
 524 License (LGPL). IPSL-CM6A-LR code (version 6.1.0) is publicly available through Apache
 525 Subversion (svn) control system, with the following command lines under Linux: `svn co`
 526 `http://forge.ipsl.jussieu.fr/igcmg/svn/modipsl/trunk modipsl; cd modipsl/util;./model`
 527 `IPSLCM6.1.11-LR` (IPSL-CM model development team, 2021). The `mod.def` file provides
 528 information regarding the different revisions used, namely (1) NEMOGCM branch
 529 `nemov36STABLE` revision 9455; (2) XIOS2 branches/`xios-2.5` revision 1873; (3) IOIPSL/src svn
 530 tags/`v224`; (4) LMDZ6 branches/`IPSLCM6.0.15` rev 3643; (5) tags/`ORCHIDEE20/ORCHIDEE`
 531 revision 6592; (6) OASIS3-MCT 2.0branch (rev 4775 IPSL server). The login and password
 532 combination requested at first use to download the ORCHIDEE component is “anonymous”
 533 and “anonymous”. We recommend referring to the project website,
 534 http://forge.ipsl.jussieu.fr/igcmg_doc/wiki/Doc/Config/IPSLCM6 (IGCMG, 2022), for a proper
 535 installation and compilation of the environment (version 6.1.10).

536

537 **Data availability**

538

539 Pollen data are available on the African Pollen Database website:
 540 <https://africanpollendatabase.ipsl.fr>. The other paleo-data are from the literature.

541

542 The IPSL-CM6A-LR model data and pre-processed model and proxies datasets used in this
 543 study are available at: <https://doi.org/10.5281/zenodo.7003853>

544

545 **Author contribution**

546

547 AML and MK designed the study. MK performed the IPSL-CM6A-LR model past1000
 548 simulations and JV the simulations analysis. MC and AML collected and analyzed the data.
 549 AML prepared the manuscript with contributions from all co-authors.

550

551 **Competing interests**

552

553 The authors declare that they have no conflict of interest

554

555 Acknowledgements

556

557 This work contributes to the ACCEDE ANR Belmont Forum project (18 BELM 0001 05). This
 558 work was undertaken in the framework of the French L-IPSL LABEX and the IPSL Climate
 559 Graduate School EUR and benefited from the FNS “SYNERGIA EffeCts of lArge voLcanic
 560 eruptions on climate and societies: UnDerstanding impacts of past Events and related
 561 subsidence cRises to evaluate potential risks in the future” (CALDERA) project under French
 562 CNRS grant agreement number CRSII5_183571 – CALDERA. MK acknowledges support from
 563 the HPC resources of TGCC under the allocations 2020-A0080107732 and 2021-A0100107732
 564 (project gencmip6) provided by GENCI (Grand Equipement National de Calcul Intensif) and
 565 2020225424 provided by PRACE (Partnership for Advanced Computing in Europe). This study
 566 benefited from the ESPRI computing and data centre (<https://mesocentre.ipsl.fr>) which is
 567 supported by CNRS, Sorbonne Université, Ecole Polytechnique and CNES as well as through
 568 national and international grants. Thanks are due to the African Pollen Database for data
 569 access. AML, MC and JV were funded by CNRS, and MK by IRD. We acknowledge the World
 570 Climate Research Programme's Working Group on Coupled Modelling.

571

572 References

- 573 Aguiar, L., Garneau, M., Lézine, A.-M., Maugis, P.: Evolution de la nappe des sables quaternaires dans
 574 la région des Niayes du Sénégal (1958-1994) : relation avec le climat et les impacts anthropiques.
 575 *Sécheresse* 21, 1-8, 10.1684/sec.2010.0237, 2010.
- 576 Aumont, O., Éthé, C., Tagliabue, A., Bopp, L., and Gehlen, M.: PISCES-v2. An ocean biogeochemical
 577 model for carbon and ecosystem studies. *Geosci. Model Develop.*, 8(8), 2465-2513,
 578 10.5194/gmd-8-2465-201, 2015.
- 579 Ballouche, A.: Dynamique des paysages végétaux sahélo-soudaniens et pratiques agro-pastorales à
 580 l'Holocène : exemples au Burkina Faso. *Bull. Asso. Géogr. Français*, 75(2), 191-200, 1998.
- 581 Bertaux, J., Sifeddine, A., Schwartz, D., Vincens, A., and Elenga, H.: Enregistrement sédimentologique
 582 de la phase sèche d’Afrique Equatoriale c. 3000 BP par la spectrométrie IR dans les lacs Sinnda et
 583 Kitina (Sud Congo). In « Dynamique à long terme des écosystèmes forestiers intertropicaux »,
 584 Paris, ORSTOM, pp. 213-215, 1998.
- 585 Boucher, O., Servonnat, J., Albright, A.L., Aumont, O., Balkanski, Y., Bastrikov, V., Bekki, S., Bonnet, R.,
 586 Bony, S., Bopp, L. et al.: Presentation and evaluation of the IPSL-CM6A-LR climate model. *J. Adv.*
 587 *Model Earth Syst.*, 12(7), e2019MS002010, 10.1029/2019MS002010, 2020.
- 588 Brncic, T.M., Willis, K.J., Harris, D.J., and Washington, R.: Culture or climate? The relative influences of
 589 past processes on the composition of the lowland Congo rainforest. *Philosoph. Trans. Royal Soc.*
 590 *B., Biol. Sci.*, 362(1478), 229-242, 10.1098/rstb.2006.1982, 2007.
- 591 Brncic, T.M., Willis, K.J., Harris, D.J., Telfer, M.W., and Bailey, R. M.: Fire and climate change impacts
 592 on lowland forest composition in northern Congo during the last 2580 years from palaeoeco-
 593 logical analyses of a seasonally flooded swamp. *Holocene*, 19, 79–89,
 594 10.1177/0959683608098954, 2009.
- 595 Carré, M., Azzoug, M., Zaharias, P., Camara, A., Cheddadi, R., Chevalier, M., Fiorillo, D., Gaye, A.T.,
 596 Janicot, S., Khodri, M., Lazar, A., Lazareth, C.E., Mignot, J., Mitma Garcia, N., Patris, N., Perrot,
 597 O., and Wade, M.: Modern drought conditions in western Sahel unprecedented in the past 1600
 598 years. *Climate Dynamics*, 52(3), 1949-1964, 10.1007/s00382-018-4311-3, 2019.
- 599 Catrain, M.: Le Petit Age de Glace en Afrique équatoriale : apport de l’étude palynologique des
 600 sédiments du lac de Petpenoun, Cameroun. Unpublished Ms Thesis. University of Paris Saclay,
 601 2021.
- 602 Coquery-Vidrovitch, C.: Écologie et histoire en Afrique noire. *Histoire, économie et société*, 483-504,
 603 1997.

- 604 Descroix, L., Diogue Niang, A., Panthou, G., Bosdian, A., Sane, Y., Dacosta, H., Malam Abdou, M.,
 605 Vandervaere, J.P., and Quantin, G.: Evolution récente de la pluviométrie en Afrique de l'Ouest à
 606 travers deux régions: la Sénégambie et le bassin du Niger moyen. *Climatologie* 12, 25-43, 2015.
- 607 d'Orgeval, T., Polcher, J., and de Rosnay, P.: Sensitivity of the West African hydrological cycle in
 608 ORCHIDEE to infiltration processes. *Hydro. Earth Syst. Sci.*, 12(6), 1387-1401, 10.5194/hess-12-
 609 1387-2008, 2008.
- 610 Demenocal, P., Ortiz, J., Guilderson, T., Adkins, J., Sarnthein, M., Baker, L., and Yarusinsky, M.: Abrupt
 611 onset and termination of the African Humid Period: rapid climate responses to gradual insolation
 612 forcing. *Quatern. Sci. Rev.*, 19(1-5), 347-361, 10.1016/S0277-3791(99)00081-5, 2000.
- 613 Deser C., Alexander, M.A., Xie, S.P., et al.: Sea surface temperature variability: Patterns and
 614 mechanisms. *Annual review of Marine Science* 2, 115–143. 10.1146/annurev-marine-120408-
 615 151453, 2010.
- 616 Elenga, H.: Végétation et climat du Congo depuis 24 000 ans B. P: analyse palynologique de séquences
 617 sédimentaires du Pays Bateke et du littoral. PhD, Aix-Marseille III, 1992.
- 618 Elenga, H., Schwartz, D., Vincens, A., Bertaux, J., de Namur, C., Martin, L., Wirrmann, D., and Servant,
 619 M.: Diagramme pollinique holocène du lac Kitina (Congo): mise en évidence de changements
 620 paléobotaniques et paléoclimatiques dans le massif forestier du Mayombe. *C. R. Acad. Sci., Série*
 621 2a, 323, 403-410, 1996.
- 622 Fofana, C.A.K., Sow, E., and Lézine, A.-M.: The Senegal River during the last millennium. *Rev. Palaeobot.*
 623 *Palynol.* 275, 104175, 10.1016/j.revpalbo.2020.104175, 2020.
- 624 Folland, C.K., Palmer, T.N., and Parker, D.E.: Sahel rainfall and worldwide sea temperatures, 1901–85.
 625 *Nature*, 320, 602–607, 10.1038/320602a0, 1986.
- 626 Gadgil, S.: The monsoon system: Land–sea breeze or the ITCZ? *J. Earth Syst. Sci.* 127, 1.
 627 10.1007/s12040-017-0916-x, 2018.
- 628 Gallego, D., Ordóñez, P., Ribera, P., Peña-Ortiz, C., and García-Herrera, R.: An instrumental index of the
 629 West African Monsoon back to the nineteenth century. *Quarter. J. Royal Meteor. Soc.*, 141(693),
 630 3166-3176, 10.1002/qj.2601, 2015.
- 631 Giannini, A., Saravanan, R., and Chang, P.: Oceanic forcing of Sahel rainfall on interannual to
 632 interdecadal time scales. *Science*, 302, 1027–1030, 10.1126/science.1089357, 2003.
- 633 Holmes, J.A., Allen, M.J., Street-Perrott, F.A., Ivanovich, M., Perrott, R.A., and Waller, M.P.: Late
 634 Holocene palaeolimnology of Bal Lake, northern Nigeria, a multidisciplinary study. *Palaeogeogr.,*
 635 *Palaeoclimatol., Palaeoecol.*, 148(1-3), 169-185, 10.1016/S0031-0182(98)00182-5, 1999.
- 636 Hourdin, F., Rio, C., Grandpeix, J.Y., Madeleine, J.B., Cheruy, F., Rochetin, N., Jam, A., Musat, I., Idelkadi,
 637 A., Fairhead, L., Foujols, M.A., Mellul, L., Traore, A.K., Dufresne, J.L., Boucher, O., Lefebvre, M.P.,
 638 Millour, E., Vignon, E., Jouhaud, J., Diallo, F.B., Lott, F., Gastineau, G., Caubel, A., Meurdesoif, Y.,
 639 and Ghattas, J.: LMDZ6A: the atmospheric component of the IPSL climate model with improved
 640 and better tuned physics. *J. Adv. Model. Earth Syst.* 12(7): e2019MS001892,
 641 10.1029/2019MS001892, 2020.
- 642 Jungclaus, J. H., Bard, E., Baroni, M., Braconnot, P., Cao, J., Chini, L. P., Egorova, T., Evans, M., Gonzalez-
 643 Rouco, J.F., Goose, H., Hurtt, G.C., Joos, F., Kaplan, J.O., Khordi, M., Goldewijk, K.K., Krivova, N.,
 644 LeGrance, A.N., Lorenz, S.J., Luterbacher, J., Man, W., Maucock, A.C., Mainshausen, M., Moberg,
 645 A., Muscheler, R., Nehbass-Ahles, C., Otto-Bliesner, B.I., Phipps, S.J., Pongratz, J., Rozanov, E.,
 646 Schmidt, G.A., Schimdt, H., Schmutz, W., Schurer, A., Shapiro, A.I., Sigl, M., Smerdon, J.E.,
 647 Solanki, S.K., Timmreck, C., Toohey, M., Usoskin, I.L.G., Wagner, S., Wu, C.J., Yeo, K.L., Zanchettin,
 648 D., Zhang, Q., and Zorita, E. : The PMIP4 contribution to CMIP6–Part 3: The last millennium,
 649 scientific objective, and experimental design for the PMIP4 past1000 simulations. *Geosci. Model*
 650 *Dev.*, 10(11), 4005-4033. 10.5194/gmd-10-4005-017, 2017.
- 651 Kageyama, M., Albani, S., Braconnot, P., Harrison, S. P., Hopcroft, P. O., Ivanovic, R. F., Lambert, F.,
 652 Marti, O., Peltier, W.R., Peterschmitt, J.Y., Roche, D.M., Tarasov, L., Zhang, X., Brady, E.C.,
 653 Haywood, A.M., LeGrande, A.N., Lunt, D.J., Mahowald, N.M., Mikolajewicz, U., Nisancioglu, K.H.,
 654 Otto-Bliesner, B.L., Renssen, H., Tomas, R.A., Zhang, Q., Abe-Ouchi, A., Bartlein, P.J., Cao, J., Li,
 655 Q., Lohmann, G., Ohgaito, R., Shi, X., Volodin, E., Yoshida, K., Zhang, X., and Zheng, W. : The

- 656 PMIP4 contribution to CMIP6—Part 4: Scientific objectives and experimental design of the
 657 PMIP4-CMIP6 Last Glacial Maximum experiments and PMIP4 sensitivity experiments. *Geosci.*
 658 *Model Dev.*, 10(11), 4035-4055, 10.5194/gmd-10-4035-2017, 2017.
- 659 Kanamitsu, M., Ebisuzaki, W., Woollen, J., Yang, S.-K., Hnilo, J.J., Fiorino, M., and Potter, G.L.: NCEP-
 660 DOE AMIP-II Reanalysis (R-2), *Bull. Amer. Meteor. Soc.*, 83, 1631-1643, 0.1175/BAMS-83-11-
 661 1631, 2002
- 662 Kucharski, F., Molteni, F., King, M.P., Farneti, R., Kang, I.S., and Feudale, L.: On the need of intermediate
 663 complexity general circulation models : A “SPEEDY” example. *Bull. Amer. Meteor. Soc.*, 94(1), 25-
 664 30, 10.1175/BAMS-D-11-00238.1, 2013.
- 665 Lawrence, D. M., Hurtt, G. C., Arneth, A., Brovkin, V., Calvin, K. V., Jones, A. D., Jones, C. D., Lawrence,
 666 P. J., de Noblet-Ducoudré, N., Pongratz, J., Seneviratne, S. I., and Shevliakova, E.: The Land Use
 667 Model Intercomparison Project (LUMIP) contribution to CMIP6: rationale and experimental
 668 design, *Geosci. Model Dev.*, 9, 2973–2998, <https://doi.org/10.5194/gmd-9-2973-2016>, 2016.
- 669 Le Borgne, J.: Un exemple d'invasion polaire sur la région mauritano-sénégalaise. *Annales Géogr.*, 489,
 670 521-548, 1979.
- 671 Lebamba, J., Vincens, A., Lézine, A.-M., Marchant, R., and Buchet, G.: Forest-savannah dynamics on the
 672 Adamawa plateau (Central Cameroon) during the “African humid period” termination : A new
 673 high-resolution pollen record from Lake Tizong. *Rev. Palaeobot. Palynol.*, 235, 129-139,
 674 10.1016/j.revpalbo.2016.10.001, 2016.
- 675 Lenton, T.M.: Early warning of climate tipping points. *Nature Climate Change* 1, 201-209,
 676 10.1038/nclimate1143, 2011.
- 677 Lézine, A.M., Lemonnier, K., and Fofana, C.A.K.: Sahel environmental variability during the last
 678 millennium: insight from a pollen, charcoal and algae record from the Niayes area, Senegal. *Rev.*
 679 *Palaeobot. Palynol.* 271, 104103, 10.1016/j.revpalbo.2019.104103, 2019.
- 680 Lézine, A.M.: Late Quaternary vegetation and climate of the Sahel. *Quatern. Res.*, 32, 317-334,
 681 10.1016/0033-5894(89)90098-7, 1989.
- 682 Lézine, A.M., Holl A., Lebamba J., Vincens A., Assi-Khadjis C., Février L., and Sultan E.: Temporal
 683 relationship between Holocene human occupation and vegetation change along the
 684 northwestern margin of the Central African rainforest. *C. R. Géosci.*, 345, 327-335,
 685 10.1016/j.crte.2013.03.001, 2013.
- 686 Lézine, A.M., Lemonnier, K., Waller, M.P., Bouimetarhan, I., Dupont, L. and APD contributors : Changes
 687 in the West African Landscape at the end of the African Humid Period. *Palaeoecology of Africa*
 688 35, 65-83, 10.1201/9781003162766-6, 2021
- 689 Lézine, A.M., Zheng, W., Braconnot, P., Krinner, G.: Late Holocene plant and climate evolution at Lake
 690 Yoa, northern Chad: pollen data and climate simulations. *Clim. Past* 7, 1351-1362, 10.5194/cp-
 691 7-1351-2011, 2011.
- 692 Maley, J., and Vernet, R. : Peuples et évolution climatique en Afrique nord-tropicale, de la fin du
 693 Néolithique à l’aube de l’époque moderne. *Afriques. Débats, Méthodes et Terrains d’Histoire*,
 694 04, 10.4000/afriques.1209, 2013.
- 695 Matthes, K., Funke, B., Andersson, M. E., Barnard, L., Beer, J., Charbonneau, P., Clilverd, M. A., Dudok
 696 de Wit, T., Haberleiter, M., Hendry, A., Jackman, C. H., Kretzschmar, M., Kruschke, T., Kunze, M.,
 697 Langematz, U., Marsh, D. R., Maycock, A. C., Misios, S., Rodger, C. J., Scaife, A. A., Seppälä, A.,
 698 Shangguan, M., Sinnhuber, M., Tourpali, K., Usoskin, I., van de Kamp, M., Verronen, P. T., and
 699 Versick, S.: Solar forcing for CMIP6 (v3.2), *Geosci. Model Dev.*, 10, 2247–2302,
 700 <https://doi.org/10.5194/gmd-10-2247-2017>, 2017.
- 701 McPhaden, M.J., Zebiak, S.E., and Glanz, M.H.: ENSO as an integrating concept in earth science.
 702 *Science*, 314, 5806, 1740-1745, 10.1126/science.1132588, 2006.
- 703 Meinshausen, M., Vogel, E., Nauels, A., Lorbacher, K., Meinshausen, N., Etheridge, D. M., Fraser, P. J.,
 704 Montzka, S. A., Rayner, P. J., Trudinger, C. M., Krummel, P. B., Beyerle, U., Canadell, J. G., Daniel,
 705 J. S., Enting, I. G., Law, R. M., Lunder, C. R., O'Doherty, S., Prinn, R. G., Reimann, S., Rubino, M.,
 706 Velders, G. J. M., Vollmer, M. K., Wang, R. H. J., and Weiss, R.: Historical greenhouse gas

- 707 concentrations for climate modelling (CMIP6), *Geosci. Model Dev.*, 10, 2057–2116,
708 <https://doi.org/10.5194/gmd-10-2057-2017>, 2017.
- 709 Mohino, E., Janicot, S., and Bader, J.: Sahel rainfall and decadal to multi-decadal sea surface
710 temperature variability. *Clim. Dyn.*, 37(3), 419–440, 10.1007/s00382-010-0867-2, 2011.
- 711 Mulitza, S., Heslop, D., Pittauerova, D., Fischer, H. W., Meyer, I., Stuetz, J. B., Zabel, M., Mollenhauer,
712 G., Collins, J.A., Kuhnert, H., and Schulz, M.: Increase in African dust flux at the onset of
713 commercial agriculture in the Sahel region. *Nature*, 466(7303), 226–228, 10.1038/nature09213,
714 2010.
- 715 Nash, D.J., De Cort, G., Chase, B.M., Verschuren, D., Nicholson, S.E., Shanahan, T.M., Asrat, A., Lézine,
716 A.M., and Grab, S.W.: African hydroclimatic variability during the last 2000 years. *Quatern. Sci.
717 Rev.*, 154, 1–22, 10.1016/j.quascirev.2016.10.012, 2016.
- 718 Ngomanda, A., Jolly, D., Bentaleb, I., Chepstow-Lusty, A., M'voubou Makaya, Maley, J., Fontune, M.,
719 Oslisly, R., Rabenkogo, N.: Lowland forest response to hydrological changes during the last 1500
720 years in Gabon, Western Equatorial Africa. *Quatern. Res.* 60, 411–425,
721 10.1016/j.yqres.2008.12.002, 2007.
- 722 Nguetsop, V. F., Bentaleb, I., Favier, C., Martin, C., Bietrix, S., Giresse, P., Servant-Vildary, M., and
723 Servant, M.: Past environmental and climatic changes during the last 7200 cal yr BP in Adamawa
724 plateau (Northern-Cameroun) based on fossil diatoms and sedimentary carbon isotopic records
725 from Lake Mbalang. *Clim. Past*, 7(4), 1371–1393, 10.5194/cp-7-1371-2011, 2011.
- 726 Nguetsop, V.F., Bentaleb, I., Favier, C., Bietrix, S., Martin, C., Servant-Vildary, S., and Servant, M.: A late
727 Holocene palaeoenvironmental record from Lake Tizong, northern Cameroon using diatom and
728 carbon stable isotope analyses. *Quatern. Sci. Rev.*, 72, 49–62, 10.1016/j.quascirev.2013.04.005,
729 2013.
- 730 Nguetsop, V.F., Servant-Vildary, S., Servant, M., and Roux, M.: Long and short-time scale climatic
731 variability in the last 5500 years in Africa according to modern and fossil diatoms from Lake Ossa
732 (Western Cameroon). *Global Planet. Change*, 72(4), 356–367, 10.1016/j.gloplacha.2010.01.011,
733 2010.
- 734 Nicholson, S.E.: The West African Sahel: A review of recent studies on the rainfall regime and its
735 interannual variability. *Intern. Scholar. Res. Not.*, 453521, 10.1155/2013/453521, 2013.
- 736 Nicholson, S.E.: Climatic variations in the Sahel and other African regions during the past five centuries.
737 *J. Arid Env.*, 1(1), 3–24, 10.1016/S0140-1963(18)31750-6, 1978.
- 738 Nicholson, S.E.: The nature of rainfall fluctuations in subtropical West Africa. *Monthly Weather Rev.*,
739 108(4), 473–487, 10.1175/1520-0493(1980)108<0473:TNORFI>2.0.CO;2, 1980.
- 740 Nicholson, S.E.: The West African Sahel: A review of recent studies on the rainfall regime and its
741 interannual variability. *Intern. Scholar. Res. Notices*, 2013, 453521, 10.1155/2013/453521,
742 2013.
- 743 Nicholson, S.E., Klotter, D., and Dezfouli, A.K.: Spatial reconstruction of semi-quantitative precipitation
744 fields over Africa during the nineteenth century from documentary evidence and gauge data.
745 *Quat. Res.*, 78, 13–23, 10.1016/j.yqres.2012.03.012, 2012
- 746 Pham-Duc, B., Sylvestre, F., Papa, F., Frappart, F., Bouchez, C. and Crétaux, J.F.: The Lake Chad
747 hydrology under current climate change. *Nature scientific Reports* 10, 5498, /s41598-020-
748 62417-w, 2020.
- 749 Reynaud-Farrera, I., Maley, J., and Wirrmann, D.: Végétation et climat dans les forêts du Sud-Ouest
750 Cameroun depuis 4770 ans BP : analyse pollinique des sédiments du Lac Ossa. *CR Acad. Sci. Paris*,
751 322(série II a), 749–755, 1996.
- 752 Rodríguez-Fonseca, B., Mohino, E., Mechoso, C. R., Caminade, C., Biasutti, M., Gaetani, M., Garcia-
753 Serrano J., Vizy E. K., Cook K., Xue Y. K., Polo I., Losada T., Druyan L., Fontaine B., Bader J., Doblas-
754 Reyes F. J., Goddard L., Janicot Serge, Arribas A., Lau W., Colman A., Vellinga M., Rowell D. P.,
755 Kucharski F., and Voltaire, A. : Variability and predictability of West African droughts: a review
756 on the role of sea surface temperature anomalies. *J. Clim.*, 28(10), 4034–4060, 10.1175/JCLI-D-
757 14-00130.1., 2015.

- 758 Rousset, C., Vancoppenolle, M., Madec, G., Fichefet, T., Flavoni, S., Barthélemy, A., Benschila, R.,
759 Chanut, J., Lévy, C., Masson, S., and Vivier, F.: The Iouvain-la-neuve sea ice model LIM3.6: global
760 and regional capabilities. *Geosci. Model. Dev.* 8(10), 2991–3005, 10.5194/gmd-8-2991-2015,
761 2015.
- 762 Salzmänn, U., and Hoelzmann, P.: The Dahomey Gap: an abrupt climatically induced rain forest
763 fragmentation in West Africa during the late Holocene. *Holocene*, 15(2), 190-199,
764 10.1191/0959683605hl799rp, 2005.
- 765 Schefuß, E., Schouten, S., and Schneider, R.R.: Climatic controls on central African hydrology during the
766 past 20,000 years. *Nature*, 437(7061), 1003-1006, 10.1038/nature03945, 2005.
- 767 Shanahan, T.M., Overpeck, J.T., Anchukaitis, K.J., Beck, J.W., Cole, J.E., Dettman, D.L., Peck, J.A., Scholz,
768 A., and King, J.W.: Atlantic forcing of persistent drought in West Africa. *Science*, 324(5925), 377-
769 380, 10.1126/science.1166352, 2009.
- 770 Street-Perrott, F.A., Holmes, J.A., Waller, M.P., Allen, M.J., Barber, N.G.H., Fothergill, P. A., Harkness,
771 D.D., Ivanovich, M., Kroon, D. and Perrott, R.A.: Drought and dust deposition in the West African
772 Sahel: a 5500-year record from Kajamarum Oasis, northeastern Nigeria. *Holocene*, 10(3), 293-
773 302, 10.1191/095968300678141274, 2000.
- 774 Tovar, C., Harris, D.J., Breman, E., Brncic, T., and Willis, K.J.: Tropical monodominant forest resilience
775 to climate change in Central Africa: A Gilbertiodendron dewevrei forest pollen record over the
776 past 2,700 years. *J. Veget. Sci.*, 30(3), 575-586, 10.1111/jvs.12746, 2019.
- 777 Toohey, M., and Sigl, M.: Volcanic stratospheric sulfur injections and aerosol optical depth from
778 500 BCE to 1900 CE, *Earth Syst. Sci. Data*, 9, 809–831, 10.5194/essd-9-809-2017, 2017.
- 779 Villamayor, J., Mohino, E., Khodri, M., Mignot, J., and Janicot, S.: Atlantic control of the late nineteenth-
780 century Sahel humid period. *J. Clim.*, 31(20), 8225-8240, 10.1175/JCLI-D-18-0148.1, 2018.
- 781 Villamayor, J., M. Khodri, S-W Fang, J. Jungclaus, C. Timmreck and D. Zanchettin: Sahel droughts
782 induced by large volcanic eruptions over the last millennium in PMIP4/past1000 simulations.
783 Submitted.
- 784 Vincens, A., Buchet, G., Elenga, H., Fournier, M., Martin, L., de Namur, C., Schwartz, D., Servant, M., and
785 Wirrmann, D.: Changement majeur de la végétation du lac Sinnda (vallée du Niari, Sud Congo)
786 consécutif à l'assèchement climatique holocène supérieur : apport de la palynologie. *C.R. Acad.*
787 *Sci. Paris*, 318, 1521-1526, 1994.
- 788 Vincens, A., Schwartz, D., Bertaux, J., Elenga, H., and de Namur, C.: Late Holocene climatic changes in
789 western equatorial Africa inferred from pollen from Lake Sinnda, southern Congo. *Quatern. Res.*
790 50(1), 34-45, 10.1006/qres.1998.1979, 1998.
- 791 Vincens, A., Schwartz, D., Elenga, H., Reynaud-Farrera, I., Alexandre, A., Bertaux, J., Mariotti, A., Martin,
792 L., Meunier, J.D., Nguetsop, F., Servant, M., Servant-Vildary, S., and Wirrmann, D.: Forest
793 response to climate changes in Atlantic Equatorial Africa during the last 4000 years BP and
794 inheritance on the modern landscapes. *J. Biogeogr.*, 26(4), 879-885, 10.1046/j.1365-
795 2699.1999.00333.x, 1999.
- 796 Waller, M.P., Street-Perrott, F.A., and Wang, H.: Holocene vegetation history of the Sahel: pollen,
797 sedimentological and geochemical data from Jikariya Lake, north-eastern Nigeria. *J. Biogeogr.*,
798 34(9), 1575-1590, 10.1111/j.1365-2699.2007.01721.x, 2007.
- 799 Wang, H., Holmes, J.A., Street-Perrott, F.A., Waller, M.P., and Perrott, R. A. Holocene environmental
800 change in the West African Sahel: sedimentological and mineral-magnetic analyses of lake
801 sediments from Jikariya Lake, northeastern Nigeria. *J. Quatern. Sci.*, 23(5), 449-460,
802 10.1002/jqs.1154, 2008.
- 803
- 804